Ocean Sci. Discuss., https://doi.org/10.5194/os-2019-43
Manuscript under review for journal Ocean Sci.
Discussion started: 17 May 2019

Ocean Science Discussions

Seasonal variation of the main tidal constituents in the Bohai Bay

Daosheng Wang[1,2], Haidong Pan[3], Guangzhen Jin[4], Xianqing Lv[3]

[1] College of Marine Science and Technology, China University of Geosciences, Wuhan 430074, China
[2] Shenzhen Research Institute, China University of Geosciences, Shenzhen 518057, China
[3] Physical Oceanography Laboratory/CIMST, Ocean University of China and Qingdao National Laboratory for Marine Science and Technology, Qingdao 266100, China
[4] School of Marine Sciences, Sun Yat-Sen University and Key Laboratory of Marine Resources and Coastal Engineering in Guangdong Province, Guangzhou 510275, China

Correspondence to: Xianqing Lv (xqinglv@ouc.edu.cn)

Abstract. The seasonal variability of the M_2 tidal amplitude has been observed widely, especially in the coastal regions, but the seasonal variations in several major tidal constituents have not been investigated sufficiently. In this study, the seasonal variations in the major tidal constituents, including M_2, S_2, K_1, and O_1, in the Bohai Bay, China, are studied by analysing one-year observations of the sea level at two stations, E1 and E2. At E2, the frequencies of the M_2 tidal amplitude and phase are annual, with large values in summer and small values in winter, while the frequencies of the S_2 and K_1 tidal amplitudes are semi-annual. Furthermore, the O_1 tidal amplitude increases constantly from winter to autumn. The maxima of the phases appear twice in one year for the S_2, K_1, and O_1 tides, which take place nearly in winter and summer. The seasonally varying trends at E1 estimated by the enhanced harmonic analysis are similar to those at E2, except for the O_1 tidal amplitude. The results of the numerical experiments indicate that the seasonality of the stratification and the corresponding vertical eddy viscosity coefficient induce seasonal variations in the phases and amplitudes for all the major tidal constituents, respectively.

1 Introduction

Although there is no primary seasonal cycle in the moon's orbit, a significant seasonal variation in the main lunar tidal constituent has been observed, which is dominant in the coastal and polar regions (Müller et al., 2014). The seasonal variation in the major tidal constituent M_2 has received considerable attention (Gräwe et al., 2014).

In several coastal regions, significant seasonal variations in the M_2 tide have been observed and investigated. Corkan (1934) inferred a seasonal modulation of the M_2 tide by analysing several sea-level records near the British coast. Foreman et al. (1995) observed the seasonal cycle in the M_2 amplitude at Victoria, which is on the southern tip of Vancouver Island off Canada's Pacific coast. Kang et al. (1995) revealed the seasonal variability of the M_2 tidal harmonic constants in the seas adjacent to Korea. Huess and Andersen (2001) found the seasonal variation in the M_2 constituent in the north-west European shelf. Kang et al. (2002) investigated the seasonal variability of the M_2 tide in the Yellow and East China Seas. Georgas (2012) observed seasonal episodes of significant tidal damping and tidal modulation in the Hudson River estuary. Müller et al. (2014) studied the global seasonal cycle of the M_2 tide and found significant seasonal variations in several coastal areas,

Ocean Sci. Discuss., https://doi.org/10.5194/os-2019-43
Manuscript under review for journal Ocean Sci.
Discussion started: 17 May 2019

e.g., North Sea, East China Sea and Yellow Sea, Sea of Okhotsk and the region of the Banda, Timor, and Arafura Seas north of Australia. Tazkia et al. (2017) found that the M_2 amplitude showed marked changes between the winter and summer seasons in the northern Bay of Bengal. Devlin et al. (2018) found that the M_2 tidal amplitude exhibited strong seasonal variability in Southeast Asia.

Furthermore, several other studies have been carried out to present and study the seasonal variability of the M_2 tide in the polar regions. Mofjeld (1986) observed the seasonal fluctuations of the tidal harmonic parameters on the north-eastern Bering Sea shelf. Kagan and Sofina (2010) showed that the seasonal variability of tidal constants was a widespread phenomenon in the Arctic Ocean. Müller et al. (2014) studied the global seasonal cycle of the M_2 tide and found significant seasonal variations in the Arctic regions.

Previous studies focused on the seasonal variation in the M_2 amplitude without considering the seasonality of other tidal constituents and their phases (Gräwe et al., 2014). In the Bohai Sea, Yellow Sea, and East China Sea, the M_2 tide has a large seasonal cycle (Müller et al., 2014), but there are few studies regarding the seasonal variability of other constituents in the Bohai Bay, which is a coastal bay in the Bohai Sea. In this study, the sea-level observations at two stations in the Bohai Bay are used to investigate the seasonal variability of the major tidal constituents, considering both the amplitude and phase. The details of the rest of the paper are as follows: the observations of sea level in the Bohai Bay and the analysis methods are described in Section 2; in Section 3, the seasonal variability of the major tidal constituents in the Bohai Bay is estimated by analysing the observations; the mechanisms for the seasonal variability of the major tidal harmonic parameters are discussed in Section 4; and the conclusions can be found in section 5.

2 Observations and methods

2.1 Observations

From 0000 UTC 1 November 2013 to 0000 UTC 1 November 2014, the total sea levels were observed hourly using the moored pressure gauge, which was accurate to within 5 cm (Lv et al., 2018), at two stations, E1 and E2, in the Bohai Bay, China (Figure 1). The time series of the total sea levels at E1 and E2 are shown in Figure 2. It is obvious that there were some gaps in the sea-level observations at E1, while the sea-level observations at E2 were covered continuously.

2.2 Classical harmonic analysis

Besides the steric sea level associated with the seawater thermal expansion, the sea level is composed of components from different sources (Kurapov et al., 2017; Lv et al., 2018):

$$\zeta(t) = \zeta_0 + \zeta_{tide}(t) + \zeta_{meteorology}(t) \quad (1)$$

where $\zeta(t)$ is the total sea level, and the three terms in the right of Equation (1) are the mean sea level, sum of the tidal components and the response of the ocean to meteorological forcing, respectively.

Ocean Sci. Discuss., https://doi.org/10.5194/os-2019-43
Manuscript under review for journal Ocean Sci.
Discussion started: 17 May 2019

The amplitude and phase of each constituent, which are subsequently termed as harmonic parameters, can be determined by analysing a time series of sea-level observations at a specific point using classical harmonic analysis (CHA). CHA can be performed using the T_Tide toolkit in MATLAB (Pawlowicz et al., 2002).

2.3 Segmented harmonic analysis

To obtain the temporally varying tidal harmonic parameters, sea-level observations are traditionally divided into several segments, and CHA is applied to each segment. The temporally varying amplitude and phase of a constituent are obtained by interpolating the discrete amplitude and phase at each segment. The aforementioned methodology is termed segmented harmonic analysis (SHA), which has been used in several previous studies (e.g., Foreman et al. (1995); Kang et al. (1995); Kang et al. (2002); Müller et al. (2014); Tazkia et al. (2017)).

In this study, the sea-level observations are divided into monthly segments according to the calendar month in SHA, as the four estimated tides, including M_2, S_2, K_1 and O_1, can be stably resolved from monthly time series. In addition, cubic spline interpolation will be used to interpolate the discrete value at each segment. Furthermore, when SHA is used, the sea-level observations are analysed only when the length of the sea-level observations for this segment is greater than 15 days.

2.4 Enhanced harmonic analysis

Through combining CHA with the independent point scheme and cubic spline interpolation, Jin et al. (2018) developed enhanced harmonic analysis (EHA) to directly obtain temporally varying tidal harmonic parameters. A MATLAB toolbox, S_TIDE, was released to realize EHA in Pan et al. (2018b). As mentioned in Pan et al. (2018b), the temporally varying harmonic parameters obtained using EHA with different numbers of independent points represented oscillations on different time scales. Therefore, the seasonal variability of the major tidal constituents will be directly obtained by using EHA with 6 independent points in this study.

3 Results

To select the estimated constituents, the sea-level observations at E1 and E2 were analysed using CHA with the consideration of nodal modulations. As a result, the four most significant constituents, including M_2, K_1, S_2 and O_1, were selected to be analysed according to the signal-to-noise ratio (Matte et al., 2013; Pawlowicz et al., 2002). In the following, the sea-level observations at E1 and E2 were analysed using CHA, SHA, and EHA by considering the M_2, K_1, S_2, and O_1 tides.

3.1 Seasonal variability at E2

As shown in Figure 3, the estimated harmonic parameters, including the temporally varying amplitude and phase, using SHA and EHA were nearly equal to each other, which were varying near those estimated using CHA, indicating that the

Ocean Sci. Discuss., https://doi.org/10.5194/os-2019-43
Manuscript under review for journal Ocean Sci.
Discussion started: 17 May 2019

temporal variations in the harmonic parameters of the major tidal constituents at E2 can be precisely obtained using both SHA and EHA. Based on Zhang et al. (2017) and Wei and Wang (2012), spring, summer, autumn, and winter were defined as March to May, June to August, September to November, and December to February of the next year, respectively. The seasonal variations of the major tidal constituents were significant (Figure 3). For the M_2 tide, the amplitude reached maximum in summer and minimum in winter, just as the phase did, which were the same as those obtained in Müller et al. (2014). There were two periods in the temporal variations of the harmonic parameters, for the S_2 tide and K_1 tide, but the trends were not similar. The maxima of the amplitude appeared in early spring and autumn for the S_2 tide, while maxima occurred in early winter and summer for the K_1 tide. On the contrary, the minima appeared in early winter and summer for the S_2 tide and early spring and autumn for the K_1 tide. The maxima of the phase for the S_2 tide were in winter and summer, while there was an approximately 1.5-month lag for the K_1 tide. Dramatically, the amplitude of the O_1 tide increased from winter to autumn, while the trend of the phase varied similarly to that for the S_2 tide.

The seasonally averaged amplitudes and phases of the major constituents are listed in Table 1. For the seasonal variations of the S_2 tidal amplitude, the trend of the averaged values was not the same as that shown in Figure 3b, as the averaged value in summer was slightly larger than that in spring. Although there was a local minimum in early summer for the S_2 tidal amplitude, in fact, the values in late summer were larger than the maximum of early spring, which resulted in the aforementioned discrepancy. A similar case appeared in the M_2 tidal phase. For other harmonic parameters of the major constituents, the trends in Table 1 varied in the same manner as those in Figure 3. The averaged M_2 tidal amplitude increased by 7.00 cm (approximately 9.47%) in summer compared to the annually averaged value and decreased by nearly 6.79 cm (approximately 9.19%) in winter, which were near the values obtained from the observations in Foreman et al. (1995) and Huess and Andersen (2001) (6%), and from the model results and observations in Müller et al. (2014) (5%–10%). For the S_2 tide, the averaged amplitudes decreased by 0.38% and 14.10% in summer and winter, respectively. On the contrary, the averaged amplitudes for the K_1 tide increased in summer and winter, in agreement with those shown in Figures 3b and 3c. The averaged O_1 tidal amplitude increased by 2.70 cm in summer compared to that in winter. Only the M_2 tidal phase in winter was less than the annually averaged value, and all of the other phases in winter and summer were larger than the annually averaged value for these four major tidal constituents.

3.2 Seasonal variability at E1

The estimated harmonic parameters of the major tidal constituents at E1 are shown in Figure 4. As there were some gaps in the sea-level observations at E1, the estimated discrete results for December 2013 and January 2014 were missing when the SHA was used, which resulted in the trends of the estimated harmonic parameters in winter differing considerably from those when the EHA was used.

To test the possible effect of the data missing at E1, the sea-level observations at E2 at the temporal positions of the missing data at E1 were deleted. The estimated harmonic parameters of the major tidal constituents, using CHA, SHA, and EHA, are shown in Figure 5. It is evident that the harmonic parameters obtained by using EHA were much closer to the

Ocean Sci. Discuss., https://doi.org/10.5194/os-2019-43
Manuscript under review for journal Ocean Sci.
Discussion started: 17 May 2019

results without considering the data missing than those using SHA, although neither of them was exactly equal to the results without the data missing. When the SHA was used, neither the local minimum during winter for the S_2 tide and the local maximum during winter for the K_1 tide was reproduced, which was successfully obtained when the EHA was used. These results indicated that the gaps in the observations had a certain influence on the estimated harmonic parameters. On the whole, the results estimated by using EHA were more reasonable.

The trends of the harmonic parameters estimated by using EHA at E1 varied similarly to those at E2, except the O_1 tidal amplitude and the M_2 tidal phase. From the averaged amplitudes and phases of the major tidal constituents at E1, listed in Table 2, an increase in the O_1 tidal amplitude of 7.22% was obtained in winter, while a reduction of 5.36% was obtained in summer. Furthermore, the averaged M_2 tidal phase in winter increased by 0.60% compared to the annually averaged value, which was contrary to that at E2. However, it could not be directly determined whether the results were correct or not, as the true values at the gaps were unknown and the oceanic environment at E1 was not the same as that at E2. Similar to those at E2, the variation in both the K_1 tidal amplitude and phase was larger than those for the other constituents.

In summary, the harmonic parameters of the major tidal constituents at E1 and E2, including amplitude and phase, exhibited significant seasonal variations. For the M_2 tide, the frequencies of the amplitudes at both E1 and E2 were annual, with large values in summer and small values in winter, which also characterised the variation of the phase at E2. The frequencies of the S_2 tidal amplitude and the K_1 tidal amplitude were semi-annual, with large (small) values in early spring (early winter) and early autumn (early summer) for the S_2 tide and in winter (early spring) and early summer (autumn) for the K_1 tide, at both E1 and E2. The O_1 tidal amplitude increased constantly from winter to autumn at E2, but there was a local maximum in winter at E1, which may be related to the data missing at E1. For the S_2, K_1 and O_1 tides, the maxima of the phase appeared twice in one year, which were nearly in winter and summer at both E1 and E2.

4 Mechanisms for the seasonal variability

Several previous studies have investigated the seasonal variability of the M_2 tidal amplitude, in which three main mechanisms have been proposed as follows:

1) Seasonal variations of the mean sea level. Corkan (1934) related the seasonal modulation of the M_2 tide near the British coast to seasonal variations of sea level and atmospheric pressure. Tazkia et al. (2017) pointed out that the seasonal variability of the sea level generated by many processes can induce a seasonal variation of the M_2 tide, as the tidal wave propagation was controlled by water depth on the first order.

2) Seasonally varying stratification. Foreman et al. (1995) presumed that the seasonal variability of the M_2 tidal amplitude at Victoria, Canada was induced by the stratification changes due to the seasonal changes in the estuarine flow. Kang et al. (2002) used a two-layer numerical model to investigate the baroclinic response of the tide and tidal currents in the Yellow and East China Seas, and found that the seasonal stratification had several noticeable effects on the tides, including varying degrees of current shear, varying frictional dissipation, and varying barotropic energy flux. Müller (2012)

indicated that in shallow seas, the seasonal variations in stratification were a major factor for the observed seasonal modulation in tides. Müller et al. (2014) pointed out that the seasonal changes in stratification on the continental shelf affected the vertical profile of the eddy viscosity to further cause the seasonal variability of the M_2 tide.

3) Seasonally varying ice coverage. St-Laurent et al. (2008) thought that the significant seasonal variations of the M_2 surface elevation in all regions of the Hudson Bay system were essentially caused by the under-ice friction. Georgas (2012) pointed out that the seasonal episodes of significant tidal damping (reductions in tidal amplitudes by as much as 50%) observed in the Hudson River estuary were primarily caused by the under-ice friction. Müller et al. (2014) found that the frictional effect between the sea-ice and surface ocean layer leaded to the seasonal variability of the M_2 tide.

Other mechanisms, including long-term changes in the tidal potential (Molinas and Yang, 1986), interactions with other physical phenomena (Huess and Andersen, 2001; Pan et al., 2018a), changes in the internal tide with corresponding small changes in its surface expression (Colosi and Munk, 2006; Ray and Mitchum, 1997) and a number of technical reasons, can also change the M_2 tidal amplitude on various time scales, which have been presented or discussed in Woodworth (2010), Müller (2012), Müller et al. (2014), and Tazkia et al. (2017).

The Bohai Sea in north China freezes to varying degrees every winter for approximately 3–4 months (Su and Wang, 2012). However, the coverage area of the sea ice is mainly concentrated in the Liaodong Bay in February 2014 during the observation period (Chen et al., 2015). Therefore, the ice coverage is not considered to be the main reason in this study. Can the first two mechanisms, indicated as the reason for the M_2 tidal amplitude in previous studies, be the cause of the seasonal variability of the harmonic parameters for the major tidal constituents, including the M_2, S_2, K_1, and O_1 tides, in the Bohai Bay? Several numerical experiments (Exp1–Exp4) were carried out to simulate the four major tidal constituents in the Bohai Sea under different conditions using MITgcm (Marshall et al., 1997) to test the influence of seasonal variations of the mean sea level and stratification on the seasonal variability of the major tidal constituents.

4.1 Design of numerical experiments

The same model settings in all the numerical experiments were described as follows. The computing area was the Bohai Sea, as shown in Figure 1. The horizontal resolution was 2′×2′. There were 16 layers in the vertical direction and the thicknesses varied from 2 m to 5 m. The four major tidal constituents, including the M_2, S_2, K_1, and O_1 tides, were implemented as tidal forcing at the east open boundary, whose information was predicted using the constant harmonic parameters extracted from the TPXO model (Egbert and Erofeeva, 2002). The surface boundary conditions were not considered. The horizontal eddy viscosity coefficient was set to 1.0×10^3 m^2/s, and the quadratic bottom drag coefficient was set to 1.3×10^{-3} (Wang et al., 2014). The integral time step was 60 s, and the total simulation time was 45 days starting from 0000 UTC 15 February 2014 in winter and 0000 UTC 15 July 2014 in summer. The results of the final fifteen days were used to calculate the harmonic parameters using the CHA.

The horizontally homogeneous profile of the initial temperature and salinity in winter and summer, as shown in Figure 6, were extracted from the HYCOM global analysis results, which were implemented for the numerical experiments in

winter and summer. To test the influence of the stratification solely, i.e., just considering the change in the temperature and salinity, the vertical eddy viscosity coefficient was specified directly, and no turbulence closure scheme was used. In Exp1 and Exp2, the vertical eddy viscosity coefficient was set to 2.0×10^{-3} m^2/s through a trial and error procedure. According to Müller et al. (2014), the eddy viscosity during summer was reduced by orders of magnitude compared to well-mixed conditions during winter, as the stratification stabilized the water column. Therefore, the vertical eddy viscosity coefficient was decreased by one-half in Exp3 to test the influence of the vertical eddy viscosity caused by the stratification. As shown in Figure 7, the monthly averaged values of the low-pass sea levels, filtered using a cosine-Lanczos filter with a high frequency cut-off of 0.8 cpd, were nearly equal to the estimated mean sea level using SHA and exhibited the same variation trend and the same order of magnitude as that of the estimated mean sea level using the EHA. The trends of the mean sea levels using SHA and EHA varied similarly: large values appeared in summer, and small values appeared in winter. According to the difference between the averaged values of the mean sea level in summer and winter, the increase in the water depth in Exp4 was set to 0.2 m to test the influence of the mean sea level. The detailed different model settings of the numerical experiments Exp1–Exp4 are listed in Table 3.

4.2 Results and discussions

The simulated harmonic parameters of the four major tidal constituents in all the numerical experiments and the results obtained from the observations, at E1 and E2, are shown in Figure 8. It was noted that the simulated harmonic parameters were a little far from the observed results, except the M_2 tidal amplitude in winter simulated in Exp1 and in summer simulated in Exp2 at E2, which may be because the constant bottom drag coefficient was used (Wang et al., 2014). However, the difference between the simulated results in different numerical experiments can be used to test the influence of the potential factors on the seasonal variability of the major tidal constituents.

As the seasonal variations of the major tidal constituents at E2 were coincident when the SHA and EHA were used, the trends in all the numerical experiments at E2 will primarily be investigated. The observed amplitudes in summer were larger than those in winter for all the four major tidal constituents, as shown in Figure 8, but the differences between the simulated amplitudes of the K_1 and O_1 tides in Exp2 and those in Exp1 decreased. On the contrary, both the decrease in the vertical eddy viscosity coefficient in Exp3 and the increase in the mean sea level in Exp4 induced the increase in the amplitude for all the major tidal constituents. The simulated results in Exp3 captured a majority of the observed change rates of the amplitude in summer to that in winter simulated in Exp1, with a factor of 2 for the M_2, S_2, and K_1 tide, which had better performance than those in Exp4, as shown in Figure 9. Therefore, the seasonal variation of the vertical eddy viscosity coefficient had a large effect on the seasonal variation of the amplitudes for all the major tidal constituents.

The differences between the simulated phases in Exp2 and Exp1 indicated that the trends in the seasonal variation of the stratification caused the same behaviour as the observed trends of the phases between summer and winter for all the major tidal constituents. The increase in the vertical eddy viscosity coefficient in Exp3 decreased the K_1 tidal phase, which was contrary to the observed trends from winter to summer. The differences between the simulated results in Exp4 and those in

Exp2 showed that the increase in the mean sea level will decrease the phases of the M_2 and K_1 tides, which was opposite of the observed results between summer and winter. The aforementioned results demonstrated that the seasonal variation in the stratification was the important mechanism for the seasonally variability of the phase for all the major tidal constituents.

The seasonal variations in all the potential factors, including the stratification, vertical eddy viscosity, and mean sea level, caused the M_2 tidal amplitude at E2 in summer to be larger than that in winter, which was consistent with the observed results. Thus, when only the M_2 tidal amplitude was considered, the conclusion about the main mechanisms were dramatically different. Although the increase in the tidal amplitude from winter to summer was smaller for the S_2, K_1 and O_1 tides than that for the M_2 tide, the change was greater than 9.72%, which was much greater than the magnitude of the variation caused by the 18.6-year nodal modulation in the observation period (less than 1%). Therefore, the seasonal variations in the four major constituents should be considered synchronously. As mentioned above, the seasonal variability of the stratification and the vertical eddy viscosity coefficient were the mechanisms responsible for the seasonal variation of the phases and amplitudes for the major tidal constituents, respectively.

Similar to those at E2, the simulated amplitudes of the four major tidal constituents in summer were larger than those in winter, as the differences between the simulated amplitudes in Exp3 and those in Exp1 were larger than 0. According to the simulated results in Exp2 and Exp1, the M_2 and K_1 tidal phases increased, and the O_1 tidal phase decreased from winter to summer, which was the same behaviour as that exhibited at E2 and opposite to the behaviour of the estimated results at E1 using EHA, further indicating that the data missing at E1 influenced the estimated results.

The variation in the amplitude for the four major constituents from winter simulated in Exp1 to summer simulated in Exp3 in the entire Bohai Sea was shown in Figure 10. It was evident that the spatial distribution of the variation in the M_2 tidal amplitude was significantly positively (R=0.98) correlated with that in the S_2 tidal amplitude, which was the same as that for the diurnal tides (R=0.96). Furthermore, the distributions were possibly related with the propagation of the tidal wave as they had similar patterns as the co-phase lines, as shown in Figure 10. For the semi-diurnal tides, including the M_2 and S_2 tides, the simulated amplitudes in summer were larger than those in winter in the Bohai Bay, the Laizhou Bay, the Liaodong Bay, and smaller than those in winter in the middle of the Bohai Sea. The spatial distribution of the absolute differences between the M_2 tidal amplitude in summer and winter had the similar pattern with that in Müller et al. (2014). For the diurnal tides, including the K_1 and O_1 tides, the simulated amplitudes in summer were larger than those in winter in the Bohai Bay, the Laizhou Bay and other southern areas, while less than those in winter in the Liaodong Bay and other northern areas.

5 Conclusions

In this study, based on one-year observations of the sea level at two stations (E1 and E2) in the Bohai Bay, China, the seasonal variability of the major tidal constituents was investigated using different methods. When the sea-level observations at E2 were analysed, the seasonal variations of all the major tidal constituents estimated by using the EHA were nearly equal

to those estimated by using SHA (Figure 3), indicating that the seasonal variations were robust and not related to the applied methods. However, the gaps in the observations at E1 had an effect on the estimated results, which was demonstrated by the experiment in which the gaps were implemented in the observation at E2 (Figure 5). At both E1 and E2, the major tidal constituents, including the M_2, S_2, K_1, and O_1 tides, exhibited significant seasonal variations. For the M_2 tide, both the large amplitude and phase were exhibited in summer, and the small values appeared in winter (Figures 3 and 4). The O_1 tidal amplitude increased constantly from winter to autumn at E2 (Figure 3d), but there was a local maximum in winter at E1 (Figure 4d), which may be related with the data missing at E1. The frequencies of all the other harmonic parameters at E1 and E2 were semi-annual, with larger values in summer and winter and small values in spring and autumn, without considering the detailed time, except the S_2 tidal amplitude. The local maxima of the S_2 tidal amplitude were in early spring and early autumn, while the local minima occurred in early winter and early summer.

Through several numerical experiments, the mechanisms of the seasonal variability of the major tidal constituents were discussed. The results showed that the seasonal variations of the phases for all the major tidal constituents were caused by the seasonality in the stratification, while the seasonality of the vertical eddy viscosity coefficient caused by the stratification resulted in the seasonal variations of the amplitudes. Therefore, the synchronous simulation of the circulation and the tides, and the reasonable parameterization scheme to convert the variations in the stratification to that in the vertical eddy viscosity were essential for the precise simulation of the tides with the consideration of the temporally varying harmonic parameters.

Data availability

The HYCOM global analysis data is available at http://hycom.org. New version of S_TIDE package can be downloaded from https://www.researchgate.net/project/Adaptation-of-tidal-harmonic-analysis-to-nonstationary-tides. The hourly sea level observations used in this work are available from the authors upon request (xqinglv@ouc.edu.cn)

Acknowledgements

This work was supported by the National Key Research and Development Program of China (Grant No. 2017YFC1404700), the Discipline Layout Project for Basic Research of Shenzhen Science and Technology Innovation Committee (Grant No. 20170418), the Guangdong Special Fund Program for Economic Development (Marine Economic) (Grant No. GDME-2018E001) and the Three Big Constructions: Supercomputing Application Cultivation Projects.

References

Chen, Y., Liu, R., and Long, h.: Change Analysis of the Spatio-temporal Characters of Sea Ice in the Bohai Sea Based on MODIS Images, Bulletin of Surveying and Mapping, 9, 83-86 (in Chinese with English abstract), 2015.

Colosi, J. A. and Munk, W.: Tales of the venerable Honolulu tide gauge, Journal of physical oceanography, 36, 967-996, 2006.

Corkan, R. H.: An Annual Perturbation in the Range of Tide, Proceedings of the Royal Society of London, 144, 537-559, 1934.

Devlin, A. T., Zaron, E. D., Jay, D. A., Talke, S. A., and Pan, J.: Seasonality of Tides in Southeast Asian Waters, Journal of Physical Oceanography, 48, 1169-1190, 2018.

Egbert, G. D. and Erofeeva, S. Y.: Efficient Inverse Modeling of Barotropic Ocean Tides, Journal of Atmospheric & Oceanic Technology, 19, 183-204, 2002.

Foreman, M. G. G., Walters, R. A., Henry, R. F., Keller, C. P., and Dolling, A. G.: A tidal model for eastern Juan de Fuca Strait and the southern Strait of Georgia, Journal of Geophysical Research Oceans, 100, 721-740, 1995.

Georgas, N.: Large seasonal modulation of tides due to ice cover friction in a midlatitude estuary, Journal of physical oceanography, 42, 352-369, 2012.

Gräwe, U., Burchard, H., Müller, M., and Schuttelaars, H. M.: Seasonal variability in M2 and M4 tidal constituents and its implications for the coastal residual sediment transport, Geophysical Research Letters, 41, 5563-5570, 2014.

Huess, V. and Andersen, O.: Seasonal variation in the main tidal constituent from altimetry, Geophysical Research Letters, 28, 567-570, 2001.

Jin, G., Pan, H., Zhang, Q., Lv, X., Zhao, W., and Gao, Y.: Determination of Harmonic Parameters with Temporal Variations: An Enhanced Harmonic Analysis Algorithm and Application to Internal Tidal Currents in the South China Sea, Journal of atmospheric and oceanic technology, 35, 1375-1398, 2018.

Kagan, B. and Sofina, E.: Ice-induced seasonal variability of tidal constants in the Arctic Ocean, Continental Shelf Research, 30, 643-647, 2010.

Kang, S. K., Chung, J.-y., Lee, S.-R., and Yum, K.-D.: Seasonal variability of the M 2 tide in the seas adjacent to Korea, Continental Shelf Research, 15, 1087-1113, 1995.

Kang, S. K., Foreman, M. G., Lie, H. J., Lee, J. H., Cherniawsky, J., and Yum, K. D.: Two-layer tidal modeling of the Yellow and East China Seas with application to seasonal variability of the M2 tide, Journal of Geophysical Research: Oceans, 107, 2002.

Kurapov, A. L., Erofeeva, S. Y., and Myers, E.: Coastal sea level variability in the US West Coast Ocean Forecast System (WCOFS), Ocean Dynamics, 67, 23-36, 2017.

Lv, X., Wang, D., Yan, B., and Yang, H.: Coastal sea level variability in the Bohai Bay: influence of atmospheric forcing and prediction, Journal of Oceanology and Limnology, doi: 10.1007/s00343-019-7383-y, 2018. Accepted, 2018.

Müller, M.: The influence of changing stratification conditions on barotropic tidal transport and its implications for seasonal and secular changes of tides, Continental Shelf Research, 47, 107-118, 2012.

Müller, M., Cherniawsky, J. Y., Foreman, M. G., and von Storch, J.-S.: Seasonal variation of the M2 tide, Ocean Dynamics, 64, 159-177, 2014.

Marshall, J., Hill, C., Perelman, L., and Adcroft, A.: Hydrostatic, quasi-hydrostatic, and nonhydrostatic ocean modeling. J Geophys Res 102(C3):5733-5752, Journal of Geophysical Research Atmospheres, 102, 5733-5752, 1997.

Matte, P., Jay, D. A., and Zaron, E. D.: Adaptation of classical tidal harmonic analysis to nonstationary tides, with application to river tides, Journal of atmospheric and oceanic technology, 30, 569-589, 2013.

Mofjeld, H. O.: Observed tides on the northeastern Bering Sea shelf, Journal of Geophysical Research: Oceans, 91, 2593-2606, 1986.

Molinas, A. and Yang, C. T.: Computer Program User's Manual for GSTARS (Generalized Stream Tube model for Alluvial River Simulation), U.S. Bureau of Reclamation Engineering and Research Center, Denver, Colorado, USA, 1986. 1986.

Pan, H., Guo, Z., Wang, Y., and Lv, X.: Application of the EMD Method to River Tides, Journal of atmospheric and oceanic technology, 35, 809-819, 2018a.

Pan, H., Lv, X., Wang, Y., Matte, P., Chen, H., and Jin, G.: Exploration of tidal-fluvial interaction in the Columbia River estuary using S_TIDE, Journal of Geophysical Research: Oceans, 123, 6598-6619, 2018b.

Pawlowicz, R., Beardsley, B., and Lentz, S.: Classical tidal harmonic analysis including error estimates in MATLAB using T_TIDE, Computers & Geosciences, 28, 929-937, 2002.

Ray, R. D. and Mitchum, G. T.: Surface manifestation of internal tides in the deep ocean: Observations from altimetry and island gauges, Progress in Oceanography, 40, 135-162, 1997.

St-Laurent, P., Saucier, F., and Dumais, J. F.: On the modification of tides in a seasonally ice-covered sea, Journal of Geophysical Research: Oceans, 113, 2008.

Su, H. and Wang, Y.: Using MODIS data to estimate sea ice thickness in the Bohai Sea (China) in the 2009–2010 winter, Journal of Geophysical Research: Oceans, 117, 2012.

Tazkia, A., Krien, Y., Durand, F., Testut, L., Islam, A. S., Papa, F., and Bertin, X.: Seasonal modulation of M2 tide in the Northern Bay of Bengal, Continental Shelf Research, 137, 154-162, 2017.

Wang, D., Liu, Q., and Lv, X.: A study on bottom friction coefficient in the Bohai, Yellow, and East China Sea, Mathematical Problems in Engineering, 2014, Article ID 432529, 2014.

Wei, S. and Wang, M.: Sea ice properties in the Bohai Sea measured by MODIS-Aqua: 2. Study of sea ice seasonal and interannual variability, Journal of Marine Systems, 95, 41-49, 2012.

Woodworth, P.: A survey of recent changes in the main components of the ocean tide, Continental Shelf Research, 30, 1680-1691, 2010.

Zhang, H., Qiu, Z., Sun, D., Wang, S., and He, Y.: Seasonal and Interannual Variability of Satellite-Derived Chlorophyll-a (2000–2012) in the Bohai Sea, China, Remote Sensing, 9, 582, 2017.

Ocean Sci. Discuss., https://doi.org/10.5194/os-2019-43
Manuscript under review for journal Ocean Sci.
Discussion started: 17 May 2019

Table 1. The averaged amplitudes (cm) and phase (°) of the major tidal constituents obtained using EHA at E2

Constituents	Parameter	Annual	Winter	Spring	Summer	Autumn
M_2	Amplitude	73.92	67.13	71.49	80.92	76.02
	Phase	210.13	209.98	209.48	212.23	209.81
S_2	Amplitude	21.07	18.10	20.81	20.99	24.34
	Phase	273.91	282.12	269.59	282.10	261.90
K_1	Amplitude	31.17	33.14	26.19	36.36	29.01
	Phase	30.94	37.61	25.96	39.13	21.14
O_1	Amplitude	24.45	22.40	24.21	25.10	26.07
	Phase	345.82	352.42	340.68	346.99	343.32

Table 2. The averaged amplitudes (cm) and phase (°) of the major tidal constituents obtained using EHA at E1

Constituents	Parameter	Annual	Winter	Spring	Summer	Autumn
M_2	Amplitude	99.94	97.23	98.47	103.89	100.11
	Phase	218.28	219.59	217.08	218.69	217.8
S_2	Amplitude	28.92	24.06	31.77	27.77	31.99
	Phase	281.06	282.31	283.64	288.09	270.11
K_1	Amplitude	34.46	40.25	29.23	38.46	29.99
	Phase	34.52	42.28	30.16	41.27	39.09
O_1	Amplitude	27.42	29.4	26.21	25.95	28.18
	Phase	349.44	354.77	345.53	349.91	347.66

Table 3. Model settings the numerical simulation experiments

No.	Season	A_z [a] (m^2/s)	Depth (m)
Exp1	Winter	2.0×10^{-3}	Original
Exp2	Summer	2.0×10^{-3}	Original
Exp3	Summer	1.0×10^{-3}	Original
Exp4	Summer	2.0×10^{-3}	Original+0.2

[a] The vertical eddy viscosity coefficient.

Ocean Sci. Discuss., https://doi.org/10.5194/os-2019-43
Manuscript under review for journal Ocean Sci.
Discussion started: 17 May 2019

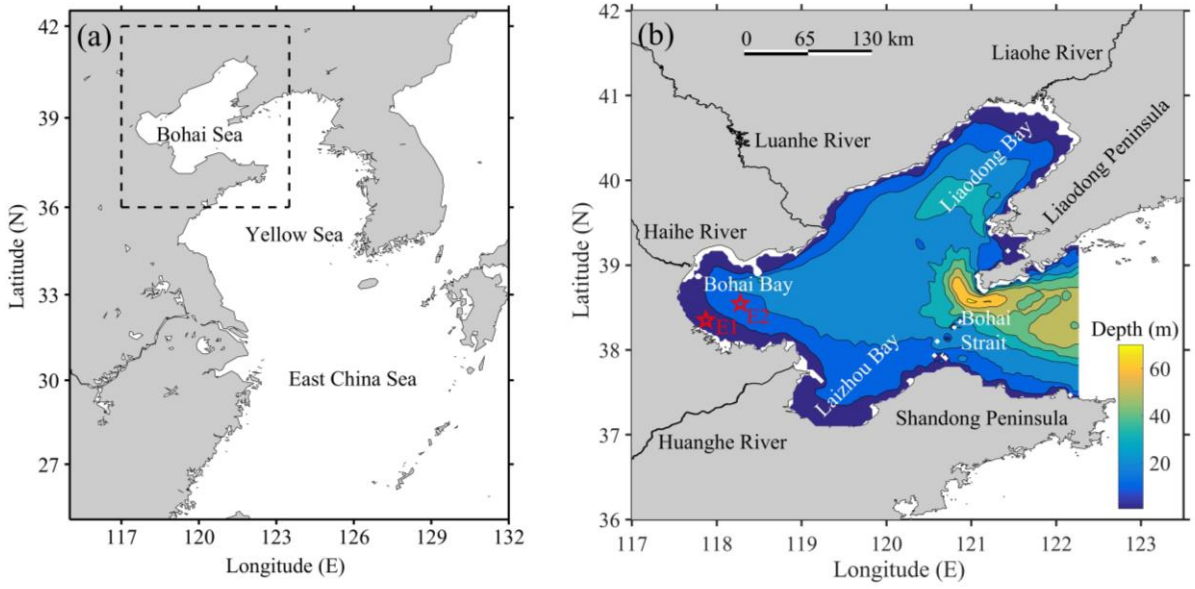

Figure 1. (a) Map showing the general location of the Bohai Sea (rectangle with dashed lines); and (b) map: location of the observation stations (red stars), E1 and E2, in the Bohai Bay, and the bathymetry of the Bohai Sea (colors).

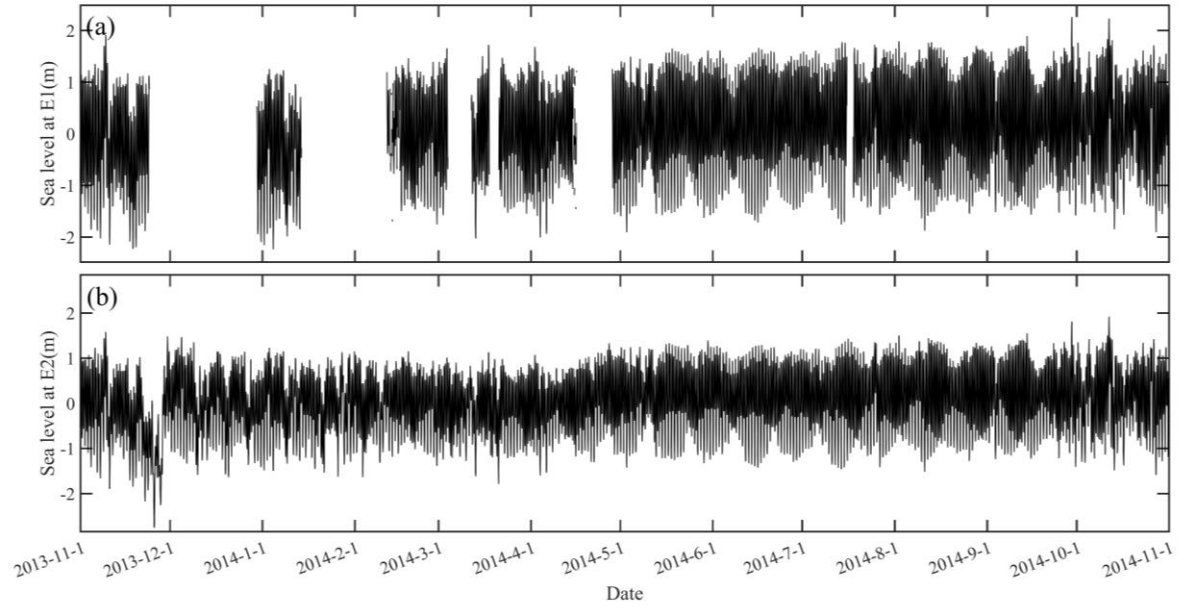

Figure 2. Time series of the observed sea level at (a) E1 and (b) E2.

Ocean Sci. Discuss., https://doi.org/10.5194/os-2019-43
Manuscript under review for journal Ocean Sci.
Discussion started: 17 May 2019

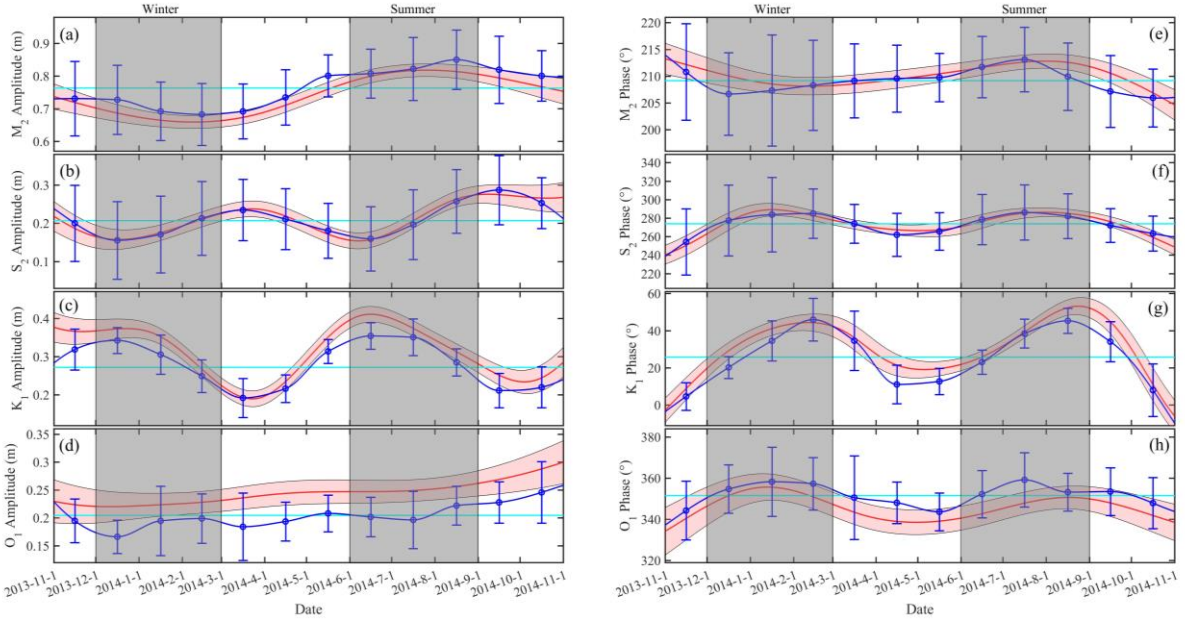

Figure 3. Time series of the estimated temporally varying tidal amplitudes of the major tidal constituents, including (a) M_2, (b) S_2, (c) K_1 and (d) O_1, at E2 when CHA (cyan lines), SHA (blue lines) and EHA (red lines) were used. (e-h) Similar to (a-d), but for the estimated temporally varying tidal phases. The blue vertical bars and the pink shadings indicate the corresponding 95% confidence intervals.

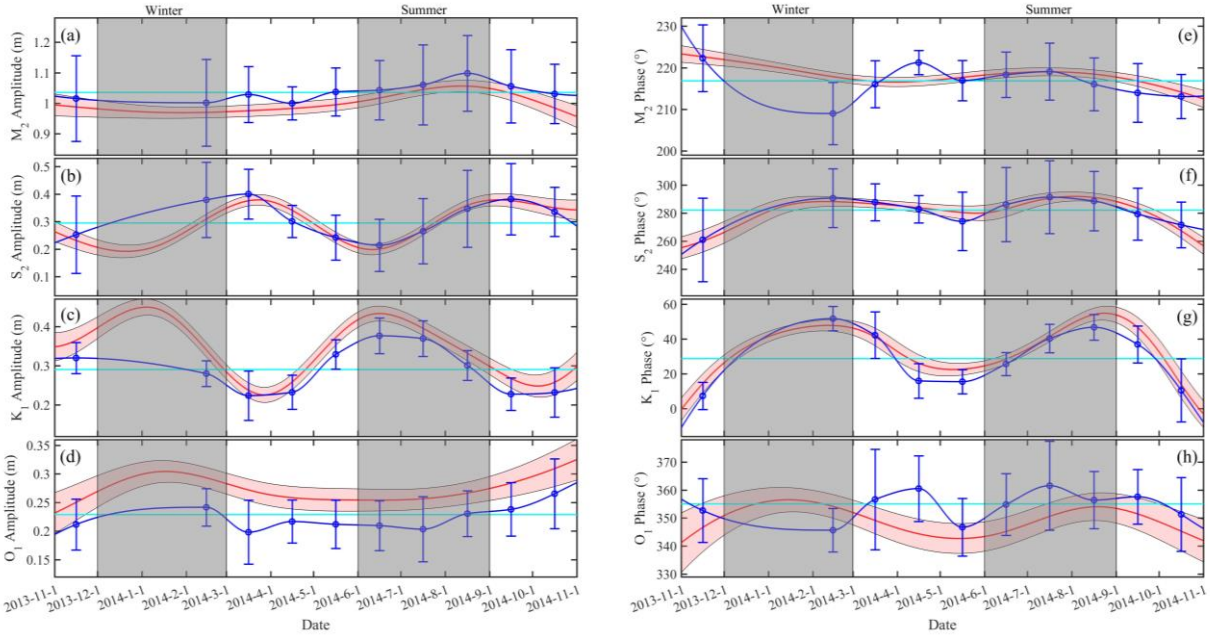

Figure 4. Similar to Figure 3, but for those at E1.

Ocean Sci. Discuss., https://doi.org/10.5194/os-2019-43
Manuscript under review for journal Ocean Sci.
Discussion started: 17 May 2019

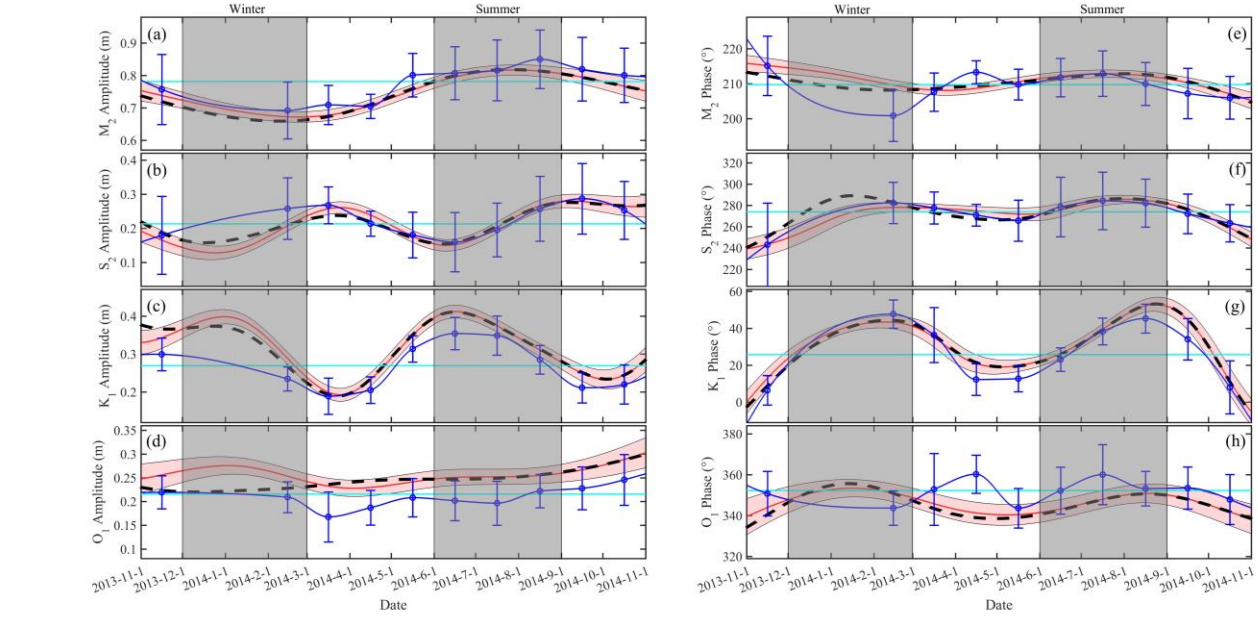

Figure 5. Time series of the estimated temporally varying tidal amplitudes of the major tidal constituents, including (a) M_2, (b) S_2, (c) K_1 and (d) O_1, at E2 when CHA (cyan lines), SHA (blue lines) and EHA (red lines) were used, when the gaps in E1 were applied in E2. (e-h) Similar to (a-d), but for the estimated temporally varying tidal phases. The black dashed lines in all the subgraphs were the results when the original observations in E2 were analysed using EHA. The blue vertical bars and the pink shadings indicate the corresponding 95% confidence intervals.

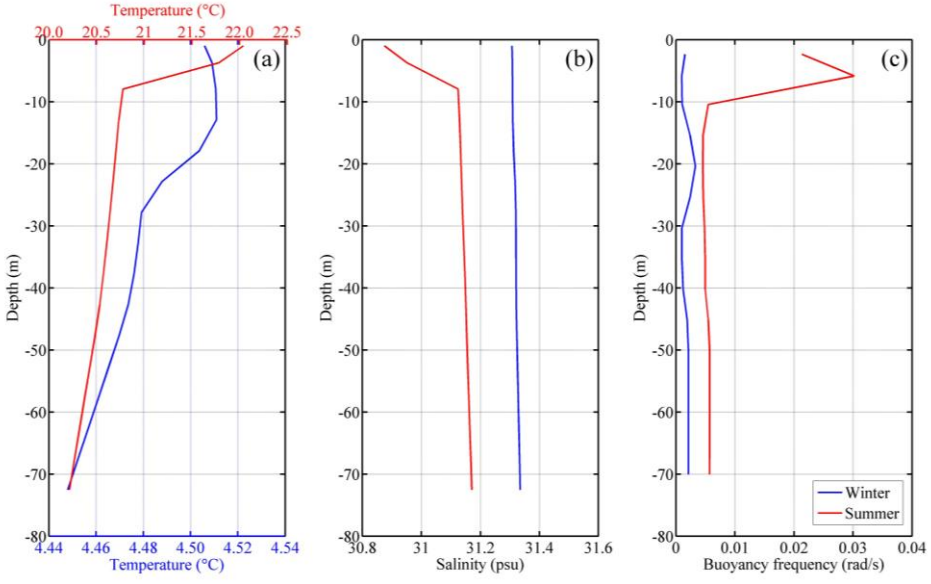

Figure 6. Horizontally homogeneous profile of the initial (a) temperature, (b) salinity and (c) buoyancy frequency used in the numerical experiments, in winter (blue solid lines) and in summer (red solid lines).

Ocean Sci. Discuss., https://doi.org/10.5194/os-2019-43
Manuscript under review for journal Ocean Sci.
Discussion started: 17 May 2019

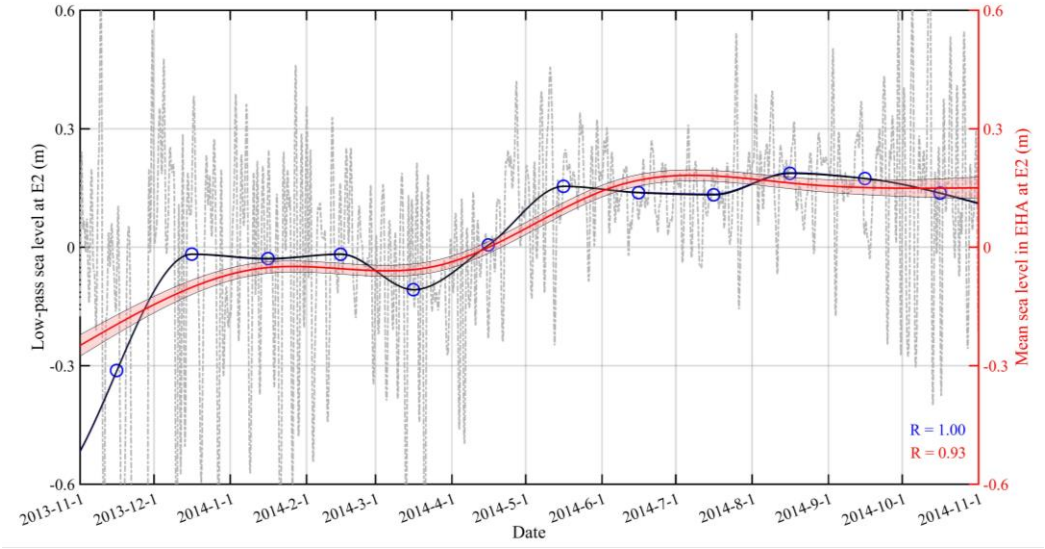

Figure 7. Time series of the original low-pass sea level (grey line), the monthly averaged values of the original low-pass sea level (blue circles), the interpolated values of the monthly averaged low-pass sea level using the cubic spline interpolation (blue line) and the estimated mean sea level using SHA (black line) and EHA (red line), at E2. It was noted that only the original low-pass sea levels with absolute values less than 0.6 m were shown and the pink shadings indicate the corresponding 95% confidence intervals.

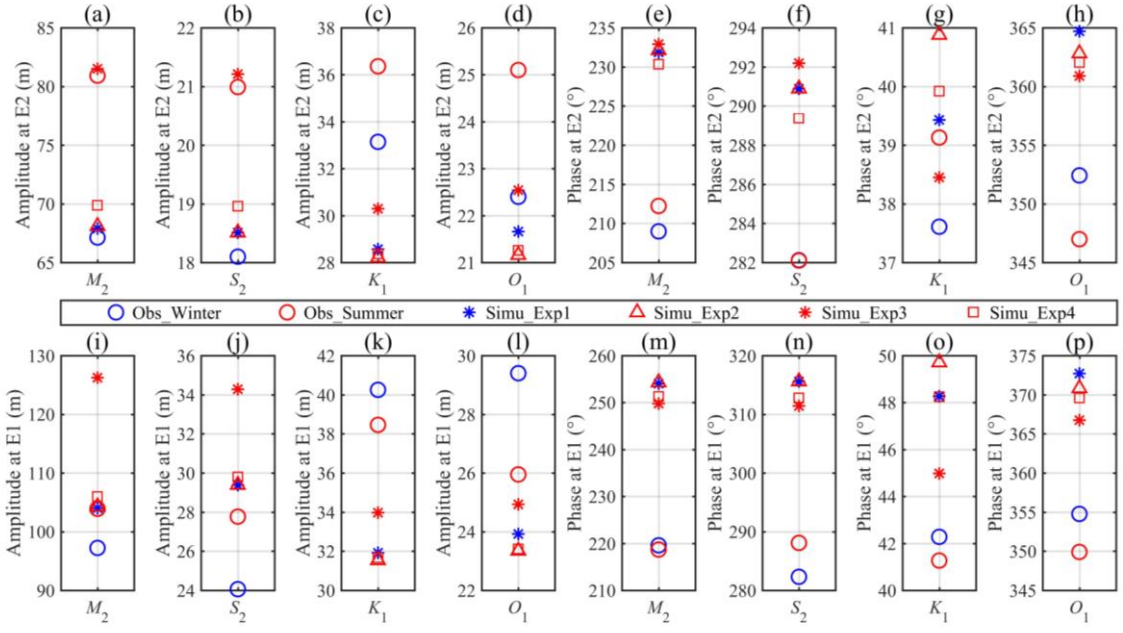

Figure 8. (a) The averaged M_2 tidal amplitude in winter (blue circle) and in summer (red circle) by analysing the observations at E2, and that obtained by analysing the simulated results in Exp1 (blue asterisk), Exp2 (red triangle),

Ocean Sci. Discuss., https://doi.org/10.5194/os-2019-43
Manuscript under review for journal Ocean Sci.
Discussion started: 17 May 2019

Exp3 (red asterisk) and Exp4 (red square). (b-d) Similar to (a), but for the S_2, K_1 and O_1 tides at E1, respectively. (e-h) Similar to (a-d), but for the phases at E2. (i-p) Similar to (a-h), but for those at E1.

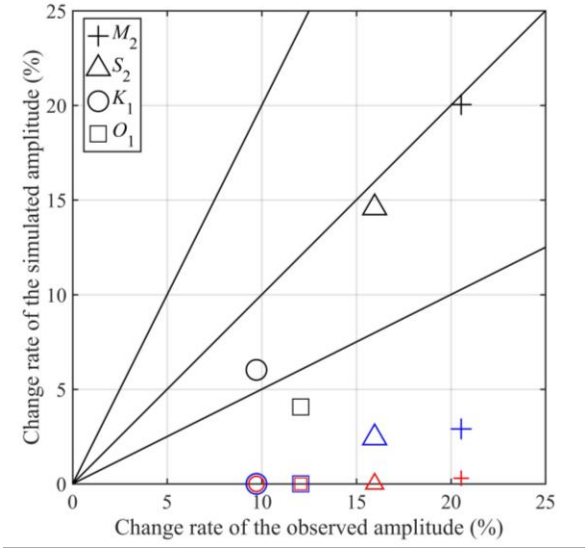

Figure 9. Comparison of simulated and observed change rate of the amplitude, for the M_2 tide (plus sign), S_2 tide (triangle), K_1 tide (circle) and O_1 tide (square), in Exp2 (red line), Exp3 (black line) and Exp4 (blue line). The 1:2, 1:2, and 2:1 lines are shown for reference. It is noted that the change rate is set to 0 when it is less than 0.

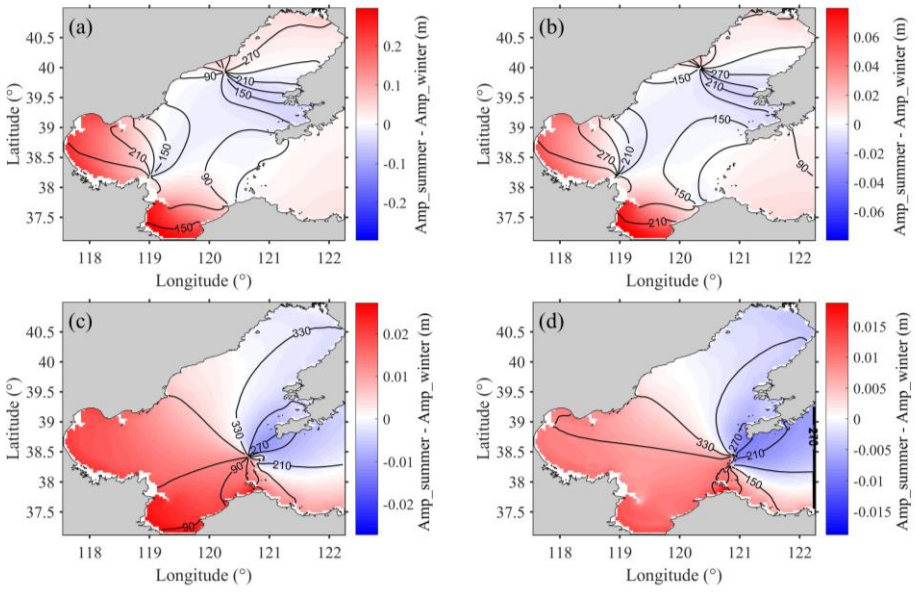

Figure 10. (a) The difference between the M_2 tidal amplitude in summer simulated in Exp3 and that in winter simulated in Exp1 (colors), and the co-phase lines of M_2 tide in winter simulated in Exp1 (black lines). (b-d) similar to (a), but for S_2, K_1 and O_1, respectively.